Chemistry
A European
Journal

Chemistry Europe
European Chemical Societies Publishing

Accepted Article

Title: Development of pH-Responsive SA/PEGDA/AS-POSS Hydrogels via Michael Addition for Controlled Drug Release and Enhanced Mechanical Properties

Authors: Yang Meng, Wen Li, Lingji Zhang, Mario Berrettoni, Hongzhong Zhang, and Xiaojing Zhang

To be cited as: *Chem. Eur. J.* **2025**, e202404538

Link to VoR: https://doi.org/10.1002/chem.202404538

WILEY VCH

10.1002/chem.202404538

Development of pH-Responsive SA/PEGDA/AS-POSS Hydrogels via Michael Addition for Controlled Drug Release and Enhanced Mechanical Properties

Yang Meng [a,&], Wen Li [a,&], Lingji Zhang [a], Mario Berrettoni [b], Hongzhong Zhang [a,*], Xiaojing Zhang [a,*]

[a] College of Materials and Chemical Engineering, Zhengzhou University of Light Industry, Henan Provincial Key Laboratory of Surface and Interface Science, Zhengzhou, PR China

[b] Department of Chemistry, University of Camerino, 62032 Camerino, Macerata, Italy

[&] These authors contributed equally to this work and should be considered co-first authors.

Abstract: In this study, thiolated sodium alginate (SA) and hydrophilic, polymerizable Janus-type polyhedral oligomeric silsesquioxane (AS-POSS) are synthesized by introducing thiol and sulfonic acid groups, respectively. A series of pH-responsive SA/PEGDA/AS-POSS nanocomposite hydrogels are successfully prepared through Michael addition reactions between the thiol groups of thiolated sodium alginate and the double bonds in the molecular chains of AS-POSS and poly(ethylene glycol) diacrylate (PEGDA). This reaction proceeds rapidly under physiological conditions without requiring initiators or catalysts. As the content of AS-POSS increases, the pore size within the hydrogel decreases, and the network structure becomes denser, with significant improvements in mechanical properties. The hydrogel exhibits excellent pH sensitivity, showing lower swelling in acidic media compared to neutral media, and undergoing hydrolysis and losing stability in alkaline media. Moreover, the incorporation of AS-POSS significantly enhances the drug-loading capacity (85.7%) and encapsulation efficiency (72.1%) of doxorubicin (DOX). The drug is released faster in weakly acidic environments, with a cumulative release rate reaching 80.4%,

demonstrating excellent targeting and controlled release properties. Cytotoxicity tests show that the SA/PEGDA/AS-POSS hydrogel has good biocompatibility and exhibits effective tumor-killing ability, indicating its great potential as a drug carrier with promising applications in biomedical materials.

Key words: Sodium alginate; Composite gel; Drug carrier; Michael addition reaction; Polyhedral oligomeric silsesquioxane.

1. Introduction

Hydrogels are soft materials with a three-dimensional polymer network structure. Due to their high water content, they exhibit excellent biocompatibility and similarity to living tissues, making them promising candidates for applications in biomaterials and biotechnology.[1] These materials typically form through the crosslinking of polymer chains in an aqueous medium, with crosslinking mechanisms including physical entanglements, ionic interactions, and chemical crosslinking.[2] Most physical gelation methods, although simple and often reversible, primarily rely on the intrinsic properties of polymers, which reduces the level of control over performance.[3] In contrast, chemical crosslinking methods allow for a more controlled and precise crosslinking process, significantly enhancing the flexibility and spatial precision of the gelation process.[4]

Common chemical crosslinking methods include free-radical crosslinking, amidation reactions, aldehyde-amine reactions, and addition reaction crosslinking.[5] Free-radical crosslinking typically relies on radical initiators to facilitate the crosslinking reactions. Although this method is rapid, it often induces undesirable side reactions, leading to structural instability or the formation of by-products.[6] Amidation reactions involves the reaction of amine groups with acidic functional groups to form stable amide bonds, enhancing the mechanical strength of the hydrogel; however, this method often requires stringent conditions, such as high temperatures or strong acidic or basic conditions, limiting its applicability. Aldehyde-amine reactions

form imine bonds through the reaction between aldehyde and amine groups, offering a straightforward approach, but incomplete crosslinking often affects the uniformity and stability of the gels.[7] In contrast, the Michael addition reaction allows nucleophilic thiol groups to react with α,β-unsaturated molecules under mild conditions, eliminating the need for initiators or catalysts. This method minimizes side reactions and can be conducted in aqueous solutions, making it ideal for the preparation of biomedical materials.[8] Hydrogels synthesized via this approach typically exceptional mechanical properties, high biocompatibility, and tunable performance, thus finding widespread application in hydrogel preparation. For example, Wu et al.[9] prepared a thiolated chitosan/methyl methacrylate-gelatin (TG) hydrogel with good antimicrobial and cell compatibility via the Michael addition reaction, which was used as a wound dressing in skin tissue engineering. Bai et al.[10] developed an injectable, degradable, and drug-releasing multifunctional chitosan/hyaluronic acid (GA-QCS/OHA) hydrogel, which effectively inhibited bacterial infection and promoted wound healing.

Sodium alginate (SA), a natural polysaccharide primarily derived from seaweed, is widely recognized for its excellent biocompatibility, biodegradability, and high solubility.[11] The carboxyl groups in its molecular structure impart notable pH responsiveness during gelation.[12] Under acidic conditions, -COO^- groups in SA chains convert to -COOH, leading to reduced ionization, polymer chain contraction, and decreased hydrophilicity. Conversely, under alkaline conditions, ionization increases, expanding the polymer chains and enhancing hydrophilicity. This pH-responsive behavior, combined with its significant functionalization potential, allows SA to be chemically modified to introduce various functional groups, thereby broadening its applications in biomedical materials. Poly(ethylene glycol) diacrylate (PEGDA), a derivative of polyethylene glycol (PEG), contains two highly reactive acrylate groups that crosslink through radical polymerization or addition reactions to form three-dimensional networks.[13] PEGDA not only demonstrates excellent water solubility but also improves the mechanical properties and stability of hydrogels through crosslinking. Its crosslinking density is adjustable, making it a versatile component in hydrogel preparation, especially for optimizing both physical and chemical properties in

biomedical applications.[14] Furthermore, the ester groups in PEGDA contribute to its biodegradability in physiological environments, making it an ideal crosslinking agent. Polyhedral oligomeric silsesquioxane (POSS), known for its stable silsesquioxane cage structure and the ability to precisely functionalize organic groups. By altering these groups at the molecular vertices, various POSS derivatives can be introduced into diverse polymer systems, significantly improving the mechanical properties and controlled drug release capabilities of hydrogels.[15] For example, Zhou et al.[16] prepared an adenine chitosan/starlike octa-arm POSS-PEG composite hydrogel loaded with silver nanoparticles via a Schiff base reaction. The incorporation of POSS improved the mechanical strength of hydrogel, self-healing properties, and cell proliferation, thereby accelerating wound healing. Li et al.[17] developed a GelMa/PNIPAM/POSS composite hydrogel through covalent bonding, which exhibited unique mechanical contraction, adhesion, and antibacterial properties, and enabled sustained exosome-controlled release to synergistically promote diabetic wound healing.

In summary, this study modifies SA and POSS by incorporating thiol functional groups and hydrophilic sulfonic acid groups into their molecular chains, enabling the successful synthesis of thiolated sodium alginate and hydrophilic, polymerizable Janus-type polyhedral oligomeric silsesquioxane (AS-POSS). Building on this, the thiol groups in the thiolated sodium alginate undergo a Michael addition reaction with the double bonds in the AS-POSS and PEGDA molecular chains, forming a pH-responsive SA/PEGDA/AS-POSS nanocomposite hydrogel. The reaction conditions are mild, allowing for rapid reaction in physiological environments without the need for initiators or catalysts. The introduction of AS-POSS not only enhances the mechanical properties of the hydrogel but also endows it with excellent drug-loading capabilities. In weakly acidic environments (such as tumor sites), the hydrogel facilitates rapid drug release with a cumulative release rate of up to 80.4%, demonstrating excellent targeting and controlled drug release ability. Additionally, the hydrogel exhibits significant cytotoxicity against liver cancer cells, indicating its promising potential as a drug carrier and its substantial value in the field of biomaterials.

2. Experimental

2.1 Reagent

Sodium alginate ($(C_6H_7O_6Na)_n$, AR, 90%), morpholine ethanesulfonic acid ($C_6H_{13}NO_4S$, AR, 99.5%), L-cysteine hydrochloride ($C_3H_7NO_2S{\cdot}HCl$, AR, 98%), N-hydroxysuccinimide ($C_4H_5NO_3$, AR, 98%), triethylamine ($C_6H_{15}N$, AR, 99.9%), doxorubicin hydrochloride ($C_{27}H_{29}NO_{11} \cdot HCl$, AR, 98%), sodium 3-mercaptopropanesulfonate ($C_3H_7NaO_3S_2$, AR, 90%), N-hydroxysuccinimide ($C_4H_5NO_3$, AR, 98%), 1-ethyl-carbodiimide hydrochloride ($C_8H_{18}CIN_3$, AR, 98%), purchased from Aladdin Chemical Reagents Co., Ltd. Concentrated hydrochloric acid (HCl, AR, 37%), anhydrous methanol (C_3H_8O, AR), concentrated sulfuric acid (H_2SO_4, AR, 70%), sodium hydroxide (NaOH, AR, 33%), sodium dihydrogen phosphate (NaH_2PO_4, AR, 99%), disodium hydrogen phosphate (Na_2HPO_4, AR, 99%), sodium chloride (NaCl, AR, 99.5%), purchased from Tianjin Fengchuan Chemical Reagent Co., Ltd. Acrylo-POSS (AR, 98%) was purchased from HYBRID, USA. Fetal bovine serum (AR), MTT thiazole blue (AR), phosphate buffer (AR), saline were purchased from Beijing Solebao Biotechnology Co., Ltd.

2.2 Sodium Alginate Thiolation Modification

Weighed 1.0 g of SA and dissolved it in 100 mL of morpholine ethanesulfonic acid solution (0.1 mol/L, pH = 6.0). Sequentially added 0.4812 g of 1-ethyl-3-(3-dimethylaminopropyl) carbodiimide hydrochloride, 0.2889 g of N-hydroxysuccinimide and adjusted the pH of the solution to 5~6 with 1 mol/L HCl. Stirred the reaction in the dark at room temperature for 15 minutes. Subsequently, added 0.3956 g of L-cysteine hydrochloride and adjusted the pH of the solution to 5 with 1 mol/L NaOH. Stirred the reaction in the dark at room temperature for 5 hours. Then, conducted dialysis in a HCl

solution with pH = 5 for 24 hours, in a 1% NaCl hydrochloric acid solution (pH = 5) for 24 hours, and subsequently in a HCl solution with pH = 5 for 48 hours. The dialysis was performed at a temperature of 4 °C and in the dark. After completing the dialysis, performed freeze-drying to obtain thiolated sodium alginate.

2.3 Synthesis of AS-POSS

A specified amount of acrylo-POSS (1321.75 g/mol) and sodium mercaptosulfonate (178.21 g/mol) were dissolved in methanol.[18] After ensuring complete dissolution, triethylamine was added, and the mixture was magnetically stirred at room temperature for 8 hours under nitrogen protection. The resulting transparent solution was concentrated using a rotary evaporator at 35 °C to remove methanol completely. The product was washed thoroughly with ethanol, dissolved in water, and subsequently freeze-dried to remove all residual water, achieving a yield of 95%.

2.4 Preparation of SA/PEGDA/AS-POSS Nanocomposite Hydrogels

The SA/PEGDA/AS-POSS nanocomposite hydrogels were prepared via the Michael addition method, and the dry gels were obtained through freeze-drying. As shown in Figure 1 and Table 1, different amounts of AS-POSS were dissolved in 2 mL of PBS solution at room temperature, and then thiolated sodium alginate and PEGDA were added, with the mixture reacted in a 37 °C constant-temperature water bath for 24 hours.

10.1002/chem.202404538

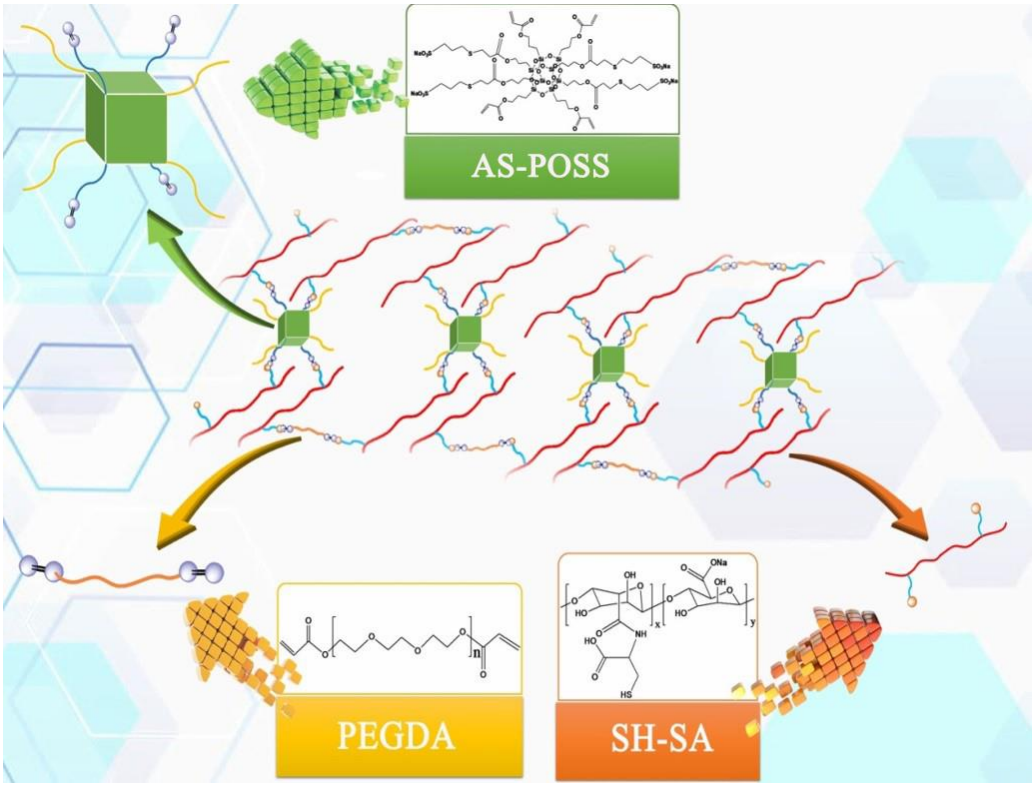

Figure 1. Schematic illustration of SA/PEGDA/AS-POSS hydrogels.

Table 1.

The preparation of SA/PEGDA/AS-POSS hydrogels.

Sample	SA (g)	PEGDA (g)	AS-POSS (g)	Gelation Time (s)	ESR
SA/PEGDA	0.12	0.20	0	289	16.9
SA/PEGDA/AS-POSS$_{30}$	0.12	0.20	0.03	193	25.8
SA/PEGDA/AS-POSS$_{60}$	0.12	0.20	0.06	166	20.3
SA/PEGDA/AS-POSS$_{90}$	0.12	0.20	0.09	138	18.7
SA/PEGDA/AS-POSS$_{120}$	0.12	0.20	0.12	125	18.6

2.5 Analysis of Microstructure and Mechanical Properties

The microstructure of the SA/PEGDA/AS-POSS composite hydrogel was characterized using FTIR and XRD. The micro morphology and element distribution of the hydrogel were analyzed through SEM and EDS. The mechanical properties were

evaluated using a rheometer for viscoelastic behavior and an electronic universal testing machine for static mechanical performance.

2.6 Swelling Performance

The hydrogel was vacuum-dried and weighed as m_1, then immersed in a PBS solution at 37 °C. At regular intervals, the gel was removed, its surface moisture wiped with filter paper, and weighed as m_2. This process was repeated until the hydrogel reached swelling equilibrium. The equilibrium swelling ratio (ESR) of the hydrogel can be calculated using the following formula (2-1):

$$SR=\frac{m_2-m_1}{m_1} \qquad (2\text{-}1)$$

Where m_1 is the mass of the dried hydrogel, and m_2 is the mass of the swollen hydrogel.

2.7 In Vitro Degradation Performance

The samples were placed in deionized water at 37 °C until their weight became constant, recorded as M_1. Then, the hydrogel samples with the initial mass M_1 were placed in buffer solutions at pH 3.0, 7.4, and 10.0 at 37 °C for degradation testing. At regular intervals, the gels were removed, their surface moisture wiped off, and their weight measured as M_2. The degradation rate of the gel can be calculated using the following formula (2-2):

$$DF=\frac{M_1-M_2}{M_1}\times 100\% \qquad (2\text{-}2)$$

M_1 is the quality of the initial hydrogel, and M_2 is the quality of the degraded hydrogel.

2.8 Drug Controlled Release Ability

The vacuum-dried hydrogel samples were placed in 10 mL of doxorubicin (DOX)

solution and soaked at room temperature for 24 hours. The supernatant was collected, and its absorbance at 480 nm was measured using a UV spectrophotometer to calculate the remaining DOX content in the solution. The soaked hydrogel was then transferred to a vacuum drying oven and dried to a constant weight to obtain drug-loaded hydrogel. The encapsulation efficiency (EE%) and drug loading (LE%) of the hydrogel were calculated using the following formulas:

$$EE=\frac{m_t-m_d}{m_t}\times 100\% \qquad (2\text{-}3)$$

$$LE=\frac{m_t-m_d}{m_0}\times 100\% \qquad (2\text{-}4)$$

Where m_0 is the initial mass of the vacuum-dried hydrogel, m_t is the initial DOX mass in the solution, and m_d is the DOX mass remaining in the solution after drug loading.

Next, pH 6.5 and 7.4 buffer solutions were prepared, and the drug-loaded hydrogels were placed in an equal volume of each buffer solution. The samples were shaken at 37 °C and 100 rpm on a constant temperature shaker. At specified time intervals, 2 mL of the solution was withdrawn, and the absorbance at 480 nm was measured using a UV spectrophotometer to determine the cumulative release of DOX. After each sample was taken, 2 mL of fresh buffer solution was added to maintain the volume. The cumulative release rate (CR) was calculated using the following formula:

$$CR=\frac{50C_i+\sum C_{(i-1)}}{m_1}\times 100\% \qquad (2\text{-}5)$$

Where C_i is the DOX concentration at each sampling point, and m_1 is the total DOX mass in the hydrogel.

2.9 Cell Compatibility

The cell viability was assessed using the MTT assay after co-culturing HepG2 (liver cancer cells) and LO2 (normal liver cells) with the samples for 48 hours.

1) Cell Culture Medium Preparation

The culture medium was prepared by mixing DMEM high-glucose medium and RPMI1640 medium with fetal bovine serum (FBS) at a ratio of 9:1.

2) Cell Culture

HepG2 and LO2 cells were cultured in a 5% CO_2, 37 °C incubator.

3) Sample Treatment

Weigh the samples and mix with RPMI1640/DMEM high-glucose culture medium containing 10% FBS at a ratio of 1:25 (weight : volume). The mixture was incubated at 37 °C for 24 hours, and the resulting extract was filtered through a 0.22 μm membrane to sterilize.

4) MTT Assay

Log-phase HepG2 and LO2 cells were counted and adjusted to the appropriate concentration, then seeded at 4×10^3 cells per well in a 96-well plate. The cells were cultured in a 5% CO_2, 37 °C incubator until they adhered to the plate. After 48 hours of treatment, the medium containing the sample was removed, and the wells were washed three times with PBS. Then, 100 μL of culture medium containing 0.5 mg/mL MTT was added, and the plate was incubated in a 5% CO_2, 37 °C incubator for 4 hours. After removing the culture medium, 100 μL of DMSO was added to each well to dissolve the formazan crystals. The absorbance at 570 nm was measured using a microplate reader.

5) Calculation of Relative Cell Viability

The relative cell viability (RGR) was calculated using the following formula:

$$RGR=\frac{OD_1}{OD_2}\times100\% \qquad (2\text{-}6)$$

Where OD_1 is the absorbance of the experimental group, and OD_2 is the absorbance of the control group.

3 Results and Discussion

3.1 Structure and Morphology of SA/PEGDA/AS-POSS Hydrogels

10.1002/chem.202404538

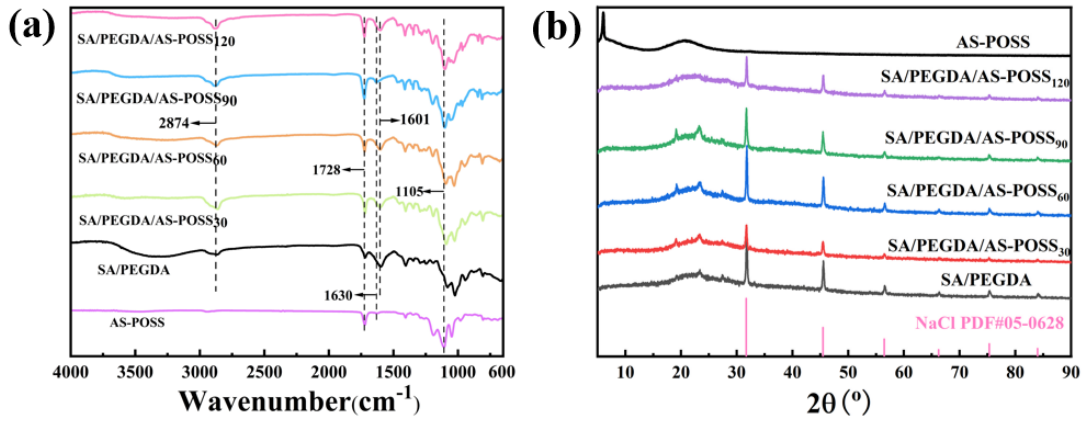

Figure 2. (a) FT-IR spectra; (b) XRD profiles of AS-POSS, SA/PEGDA and SA/PEGDA/AS-POSS hydrogels.

Figure 2(a) presents the infrared spectra of AS-POSS, SA/PEGDA, and SA/PEGDA/AS-POSS hydrogels. A characteristic absorption peak corresponding to the stretching vibration of the carbonyl group (C=O) is observed around 1728 cm^{-1}. The absorption peak at 1105 cm^{-1} is attributed to the Si-O-Si stretching vibration in AS-POSS, while the C-H stretching vibration appears at 2874 cm^{-1}. Additionally, the carboxyl group ($-COO^-$) exhibits a stretching vibration peak near 1601 cm^{-1}. Notably, the characteristic peaks for the carbon-carbon double bond (C=C) stretching at 1630 cm^{-1} and the thiol group (S-H) stretching at 2556 cm^{-1} are absent in the IR spectra of SA/PEGDA and SA/PEGDA/AS-POSS hydrogels. This confirms that a Michael addition reaction has taken place between the thiolated sodium alginate, AS-POSS, and PEGDA. The XRD spectra of SA/PEGDA and SA/PEGDA/AS-POSS hydrogels (Figure 2(b)) display prominent diffraction peaks at 31.7°, 45.6°, and 56.6°, suggesting the presence of crystalline regions within the hydrogel. Upon further analysis, these diffraction peaks are attributed to NaCl crystals formed inside the hydrogel network. The NaCl crystals result from the ionization of $-SO_3Na$ groups in the AS-POSS molecular chains, which combine with Na^+ from the buffer solution and Cl^- from the same solution through covalent bonding to form NaCl crystals.

10.1002/chem.202404538

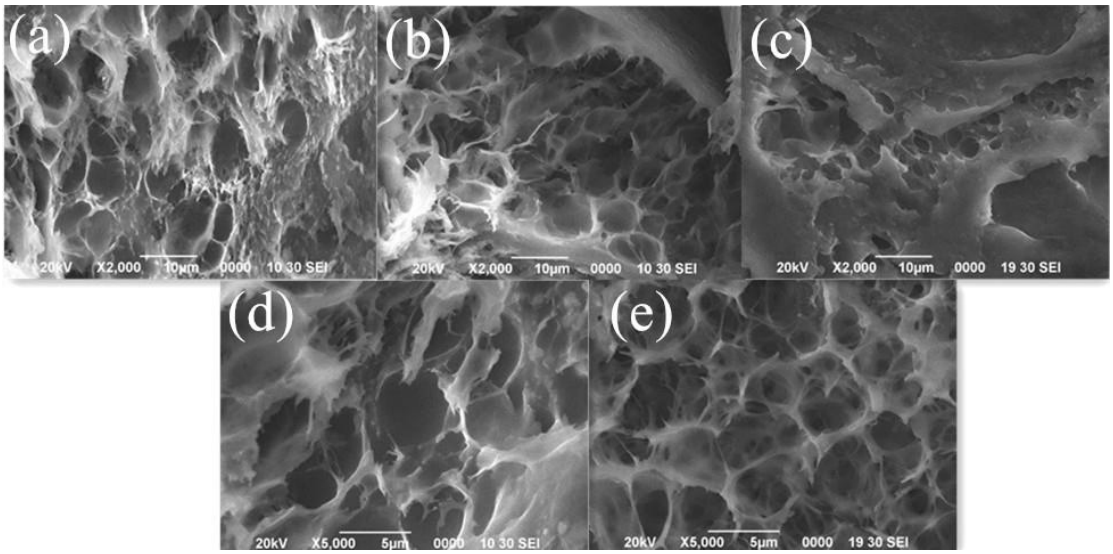

Figure 3. SEM images of hydrogels: (a) SA/PEGDA; (b) SA/PEGDA/AS-POSS$_{30}$; (c) SA/PEGDA/AS-POSS$_{60}$; (d) SA/PEGDA/AS-POSS$_{90}$; (e) SA/PEGDA/AS-POSS$_{120}$.

The microstructure and elemental distribution of SA/PEGDA/AS-POSS hydrogels were examined using SEM and EDS. As shown in Figure 3, the pore distribution across the hydrogel is relatively uniform. The SA/PEGDA hydrogel exhibits the largest pore size, approximately 8 μm, as the AS-POSS content increases, the pore size of the hydrogel decreases. The SA/PEGDA/AS-POSS$_{120}$ hydrogel, for example, displays a pore diameter of around 3 μm. This reduction in pore size is attributed to the increased AS-POSS content, which enhances the number of crosslinking points within the gel network, resulting in a denser structure and a shorter gelation time. Furthermore, the Si element within the hydrogel is evenly distributed (Figure S1) without significant aggregation, demonstrating that AS-POSS exhibits clear advantages in terms of compatibility with polymer matrices, compared to conventional nanoparticles that are prone to aggregation. Figure4 illustrates the macroscopic appearance of the hydrogel, highlighting its excellent moldability and injectability.

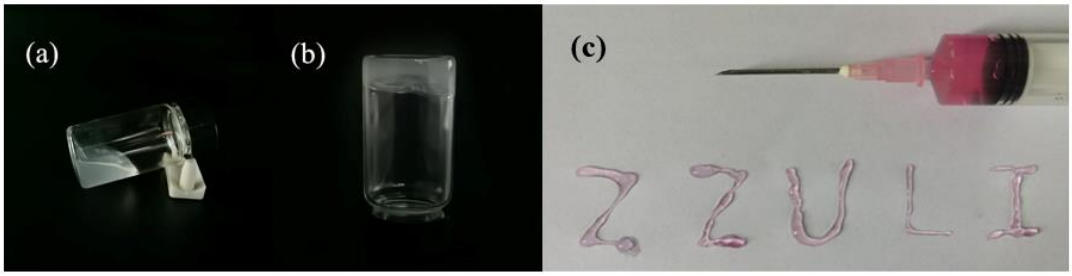

Figure 4. Gel process: (a) before gelation; (b) after gelation; (c) the appearance of the injection SA/PEGDA/AS-POSS$_{120}$ hydrogel.

3.2 Rheological Behavior and Compression Properties of SA/PEGDA/AS-POSS Hydrogels

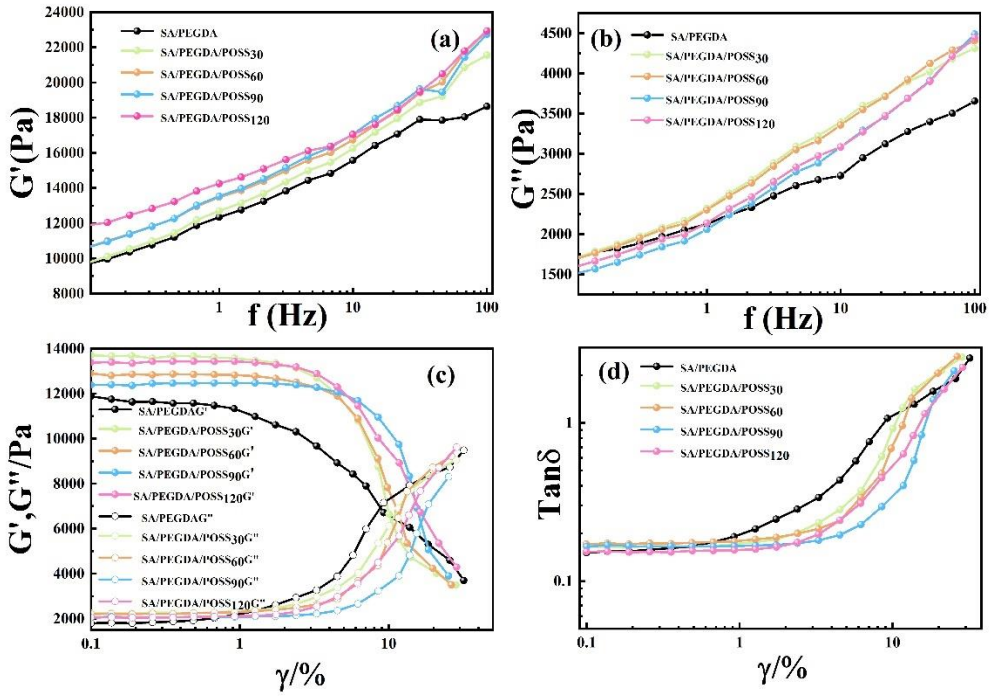

Figure 5. Rheological behavior curves of SA/PEGDA/AS-POSS hydrogels: (a) and (b) different frequencies; (c) and (d) different strain.

To investigate the effect of AS-POSS content on the rheological behavior of hydrogels, rheological tests were conducted on SA/PEGDA/AS-POSS hydrogels. Figure 5(a) and (b) show the variation of elastic modulus (G') and viscous modulus

(G'') with frequency. With increasing AS-POSS content, the elastic modulus of the SA/PEGDA/AS-POSS hydrogels gradually increases. The viscous modulus is also consistently higher than that of the SA/PEGDA hydrogel within a certain frequency range. Figure 5(c) and (d) illustrate the changes in elastic modulus, viscous modulus, and loss factor (tan δ) as a function of strain amplitude at a frequency of 1 Hz. As strain increases, the elastic modulus and viscous modulus of the SA/PEGDA/AS-POSS hydrogels intersect, which corresponds to the yield strain point. This intersection demonstrates the collapse of the three-dimensional network structure of the hydrogel under strain. Within a certain range, the yield strain increases with increasing AS-POSS content, suggesting that the introduction of AS-POSS enhances the crosslinking points and the crosslinking density of the hydrogel, thereby improving structural stability and elasticity of the hydrogel. The loss factor, defined as the ratio of viscous modulus to elastic modulus, reflects the viscoelastic behavior of the hydrogel. A higher loss factor denotes greater viscosity, while a lower value reflects greater elasticity. As shown in Table 2, the loss factor of SA/PEGDA/AS-POSS hydrogels exhibit a higher loss factor compared to SA/PEGDA hydrogel, indicating that the incorporation of AS-POSS enhances the viscosity of the hydrogel to some extent.

Table 2.

Rheological and compression properties of SA/PEGDA/AS-POSS hydrogels.

Sample	Yield strain (%)	Loss factor	Compressive strain (%)	Compressive strength (kPa)	Compressive modulus (kPa)
SA/PEGDA	8.8	0.15	39.2	2.3	5.5
SA/PEGDA/AS-$POSS_{30}$	10.4	0.16	43.5	5.2	15.5
SA/PEGDA/AS-$POSS_{60}$	11.8	0.17	54.5	10.1	23.6
SA/PEGDA/AS-$POSS_{90}$	16.6	0.17	49.5	9.8	26.2

SA/PEGDA/AS-POSS$_{120}$	15.5	0.16	70.1	12.4	50.1

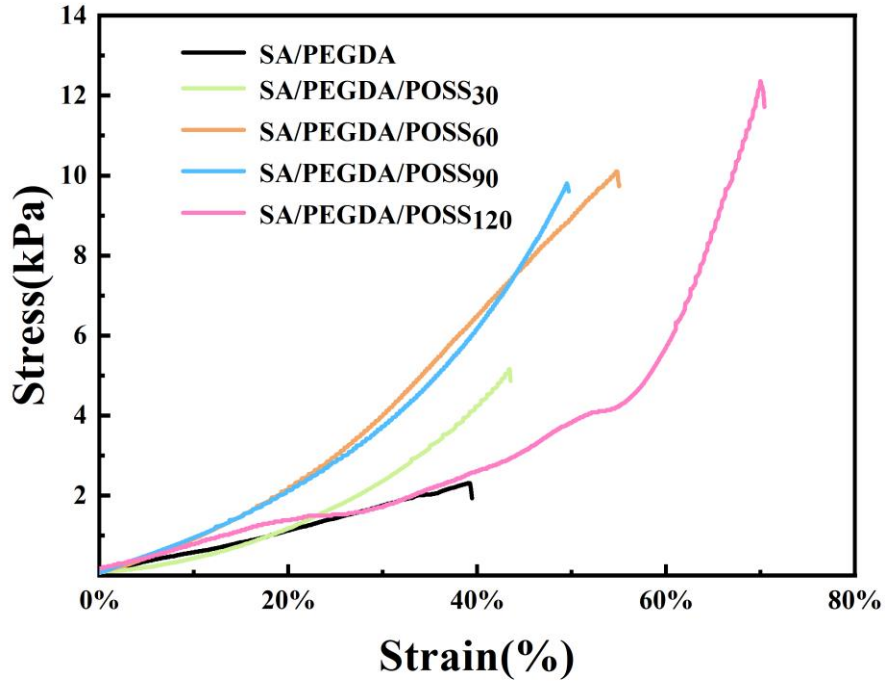

Figure 6. Compression properties of SA/PEGDA/AS-POSS hydrogels.

The compression properties of SA/PEGDA/AS-POSS hydrogels were assessed to analyze the influence of AS-POSS content on mechanical performance, as presented in Figure 6. The SA/PEGDA hydrogel exhibits a compression strain of 39.8% and a compression strength of 2.3 kPa. With the addition and increasing content of AS-POSS, both compression strain and compression strength show significant enhancement. For instance, the SA/PEGDA/AS-POSS$_{120}$ hydrogel achieves the highest compression strain and strength, reaching 70.1% and 12.4 kPa, respectively. Furthermore, the compression modulus (Table 2) continuously increases with rising AS-POSS content. These results clearly demonstrate that the introduction of AS-POSS significantly enhances the compression properties of the hydrogel. This improvement aligns with the rheological results, further validating the positive impact of AS-POSS on the mechanical properties of hydrogels.

10.1002/chem.202404538

3.3 Swelling Properties of SA/PEGDA/AS-POSS Hydrogels

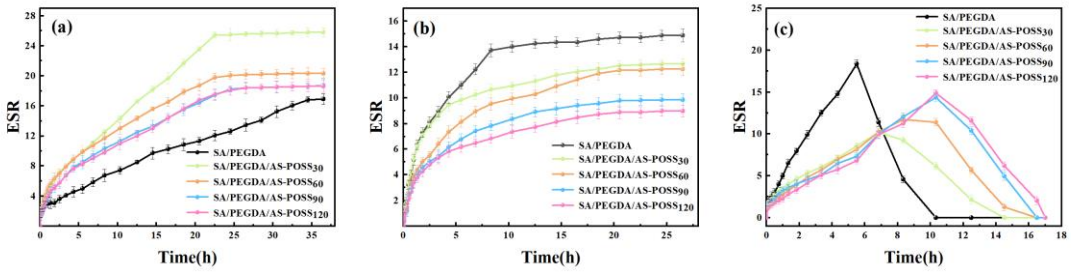

Figure 7. Swelling performance of SA/PEGDA/AS-POSS hydrogels at 37 ºC: (a) pH=7.4; (b) pH=3.0; (c) pH=10.0.

Figure 7 (a), (b), and (c) present the swelling behavior of SA/PEGDA/AS-POSS hydrogels at 37 °C in different pH environments (pH = 7.4, pH = 3.0, and pH = 10.0). In neutral conditions (Figure 7(a)), the SA/PEGDA hydrogel reaches equilibrium swelling after approximately 35 hours, with the slowest swelling rate with an equilibrium swelling ratio of 16.4. In contrast, the swelling rate and equilibrium swelling ratio of SA/PEGDA/AS-POSS hydrogels significantly increase. As the AS-POSS content rises, the equilibrium swelling ratio initially increases and then decreases. This trend is due to the enhanced hydrophilicity provided by sulfonic acid groups introduced by AS-POSS, which improves swelling properties of the hydrogel. However, with further increase in AS-POSS content, the crosslinking density of the hydrogel increases, forming a tighter network structure with smaller pore size, which reduces the swelling capacity of the hydrogel. In acidic conditions (Figure 7(b)), the equilibrium swelling ratios of all hydrogels are lower than in neutral conditions. At lower pH, the carboxyl groups in sodium alginate exist in a non-ionized state, reducing the hydrophilicity of the polymer, causing the molecular chains to shrink and collapse. Furthermore, the incorporation of AS-POSS increases crosslinking density, leading to a more compact pore structure and further reducing swelling capacity. In alkaline conditions (Figure 7(c)), the hydrogel swell initially, reaching their maximum swelling degree before degradation. The swelling rate in alkaline solution surpasses than that in

neutral and acidic solutions. This occurs due to the increased ionization of the carboxyl groups under alkaline conditions, which enhances the hydrophilicity of the polymer, allowing more water molecules to enter. Subsequently, the ester groups in the polymer undergo hydrolysis and cleavage, leading to rapid degradation of the hydrogel. As the AS-POSS content increases, the time to reach maximum swelling gradually lengthens. This effect arises from the stabilizing influence of AS-POSS on the network structure, which slows the rate at which water molecules penetrate and delays the degradation process. In summary, SA/PEGDA/AS-POSS hydrogels exhibit excellent pH responsiveness, with a significantly lower equilibrium swelling ratio in acidic media compared to neutral media, and instability in alkaline conditions.

3.4 Degradation of SA/PEGDA/AS-POSS Hydrogels In Vitro

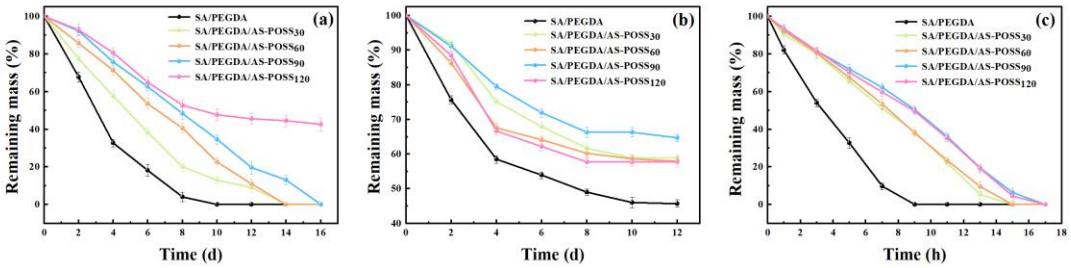

Figure 8. Degradation performance of SA/PEGDA/AS-POSS hydrogels at 37 ºC: (a) pH=7.4; (b) pH=3.0; (c) pH=10.0.

Figure 8 (a), (b), and (c) show the degradation performance of SA/PEGDA/AS-POSS hydrogels at 37 °C in different pH environments (pH = 7.4, pH = 3.0, and pH = 10.0). Under neutral conditions (Figure 8(a)), the SA/PEGDA hydrogel degrades the fastest, completely degrading within 9 days. This rapid degradation can be attributed to its single-network structure and large pores, allows water molecules to easily penetrate, accelerating the hydrolysis of ester groups and thus speeding up the degradation process. As the AS-POSS content increases, the degradation rate of SA/PEGDA/AS-POSS hydrogels gradually slows down. Notably, the SA/PEGDA/AS-POSS$_{120}$ hydrogel retains 42.6% of its initial mass after 16 days, while the other hydrogels undergo

10.1002/chem.202404538

complete degradation within the same period. These findings indicate that the introduction of AS-POSS significantly reduces the degradation rate of the hydrogels, and the degradation time can be controlled by adjusting the AS-POSS content. As shown in Figure 8(b), the degradation rate of the hydrogels under acidic conditions is lower than that under neutral conditions, reaching equilibrium after approximately 12 days. The addition of AS-POSS further slows the degradation rate, with the remaining mass of all SA/PEGDA/AS-POSS hydrogels being above 57%, demonstrating that AS-POSS enhances the stability of the hydrogels in acidic conditions. This effect arises because, in acidic conditions, carboxyl groups on the molecular chains remain in a non-ionized state, reducing hydrophilicity, causing molecular chains to contract, and limiting water penetration. Additionally, AS-POSS strengthens the network structure, reduces pore size, and slows water molecule ingress, thereby restricting the hydrolysis of ester bonds and lowering the degradation rate in acidic conditions. Under alkaline conditions (Figure 8(c)), the hydrogels degrade rapidly, with complete degradation occurring within 17 hours, while the introduction of AS-POSS effectively slows this process. Overall, SA/PEGDA/AS-POSS hydrogels exhibit excellent pH responsiveness, with the degradation rate being modulated by the amount of AS-POSS incorporated, which is consistent with their swelling behavior.

3.5 Drug Release Properties of SA/PEGDA/AS-POSS Hydrogels

10.1002/chem.202404538

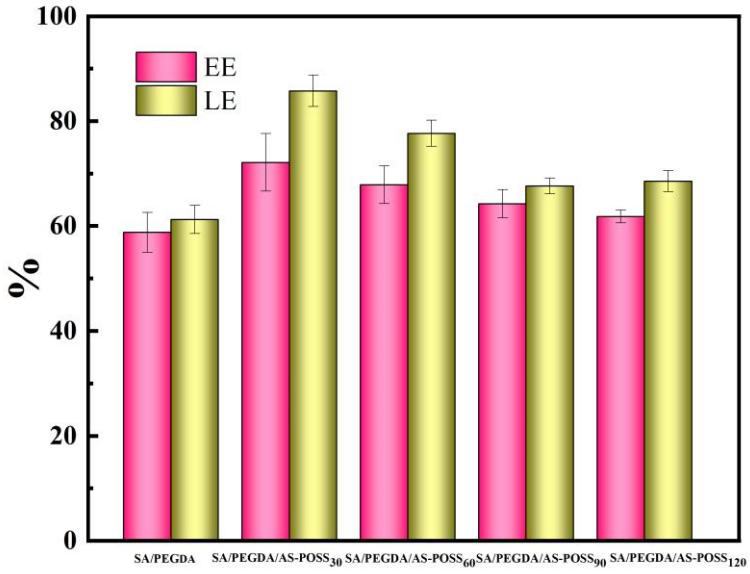

Figure 9. Encapsulation efficiency and drug loading efficiency of SA/PEGDA/AS-POSS hydrogels.

Due to their porous structure, excellent hydrophilicity, and relatively stable network, hydrogels can effectively control drug release, making them ideal as drug carriers with promising therapeutic outcomes.[19] As demonstrated in the previous experiments, SA/PEGDA/AS-POSS hydrogels exhibit exceptional pH responsiveness, and the pH value in tumor regions of the human body is lower than that of normal cells (pH = 7.4), creating a mildly acidic environment.[20] This property enables SA/PEGDA/AS-POSS hydrogels to be used as drug carriers for controlled drug release. Based on the structure of SA/PEGDA/AS-POSS hydrogels, doxorubicin hydrochloride (DOX) was selected as the model drug. This choice stems from the water solubility of DOX, which facilitates its diffusion into the hydrogel along with water molecules. Furthermore, the amino ($-NH_2$) groups of DOX undergo protonation, becoming positively charged and forming electrostatic interactions with $-COO^-$ and $-SO_3^-$ groups on the molecular chains of the hydrogel. These interactions enable DOX molecules to be effectively adsorbed within the hydrogel network, imparting it with a certain drug-loading capacity.

As shown in Figure 9 and Table 3, the encapsulation efficiency (EE) of SA/PEGDA hydrogel reaches 58.8%, with a drug loading efficiency (LE) of 61.2%.

The introduction of AS-POSS significantly enhances both the encapsulation and drug loading capacities. For instance, SA/PEGDA/AS-POSS$_{30}$ hydrogel achieves an encapsulation efficiency of 72.1% and a drug loading efficiency of 85.7%. This improvement can be attributed to the sulfonic groups on the molecular chains of SA/PEGDA/AS-POSS, which increase the hydrophilicity of the polymer, facilitating the diffusion of more DOX molecules into the hydrogel with water. Additionally, the sulfonic groups, acting as electron-withdrawing groups, enable electrostatic interactions with DOX, further boosting the drug loading capacity. However, as the content of AS-POSS increases, the drug loading capacity slightly decreases. This decrease results from the increasingly dense network structure of the hydrogel, which reduces the swelling ratio and limits the diffusion of DOX into the interior of the hydrogel along with water molecules. Although the number of sulfonic groups increases, the compact network structure hinders the penetration of DOX molecules, causing more DOX to be adsorbed onto the surface of the hydrogel.

Table 3.

Drug sustained-release properties of SA/PEGDA/AS-POSS hydrogels.

Sample	EE (%)	LE (%)	pH=6.5CR (%)	pH=7.4CR (%)
SA/PEGDA	58.8	61.2	80.6	42.2
SA/PEGDA/AS-POSS$_{30}$	72.1	85.7	81.3	39.1
SA/PEGDA/AS-POSS$_{60}$	67.9	77.6	70.8	34.1
SA/PEGDA/AS-POSS$_{90}$	64.2	67.6	68.7	28.8
SA/PEGDA/AS-POSS$_{120}$	61.8	68.5	68.3	30.2

10.1002/chem.202404538

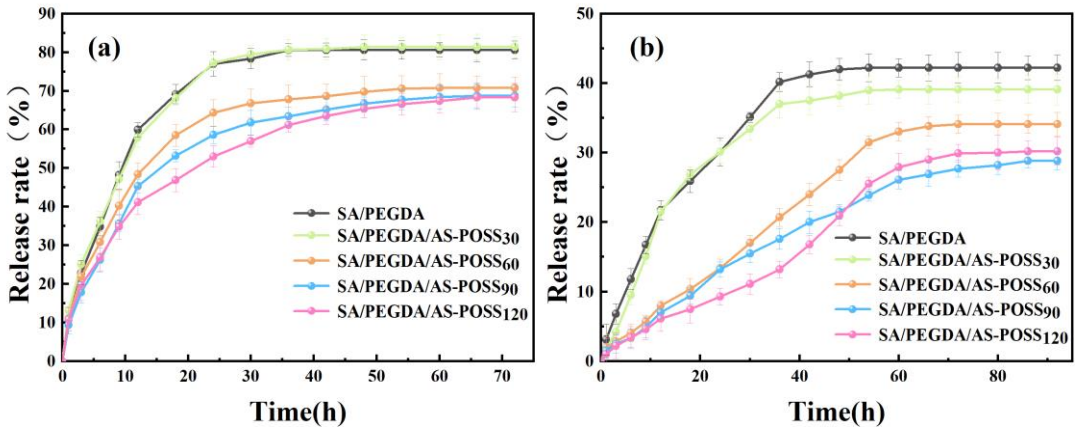

Figure 10. The cumulative release rate of SA/PEGDA/AS-POSS hydrogels in 37 ºC PBS solution: (a) pH=6.5; (b) pH=7.4.

The drug release performance of SA/PEGDA/AS-POSS hydrogels in PBS buffer at different pH values (pH = 6.5 and pH = 7.4) at 37 °C was further investigated, as shown in Figure 10. In the weakly acidic environment (pH = 6.5) (Figure 10(a)), the DOX in the hydrogel releases rapidly within 25 hours, with the cumulative drug release rate reaching its highest at 81.3% for the SA/PEGDA/AS-$POSS_{30}$ hydrogel. In contrast, in the neutral environment (pH = 7.4) (Figure 10(b)), the release of DOX is slower, with a cumulative release rate of 36.1% for the SA/PEGDA/AS-$POSS_{30}$ hydrogel after 60 hours. This difference can be attributed to the fact that in the acidic environment, a higher concentration of H^+ ions interacts with the $-COO^-$ and $-SO_3^-$ groups within the molecular chains of the hydrogel, reducing the adsorption of DOX molecules, making it easier for DOX to be released, thus enhancing the drug release rate in the acidic environment. Additionally, the drug release mechanism of the hydrogel was investigated (Table S1-4). In the weakly acidic environment (pH = 6.5), the drug release process of DOX closely follows the Ritger-Peppas kinetic model. Based on the Ritger-Peppas model, the diffusion exponent (n) was calculated to be less than 0.45, indicating that the drug release mechanism of DOX in SA/PEGDA/AS-POSS hydrogels follows Fickian diffusion. In the neutral pH environment (pH = 7.4), the drug release mechanism of DOX in SA/PEGDA/AS-POSS hydrogels follows non-Fickian diffusion,

10.1002/chem.202404538

involving a combined process of diffusion and erosion.

3.6 Cell Compatibility of SA/PEGDA/AS-POSS Hydrogels

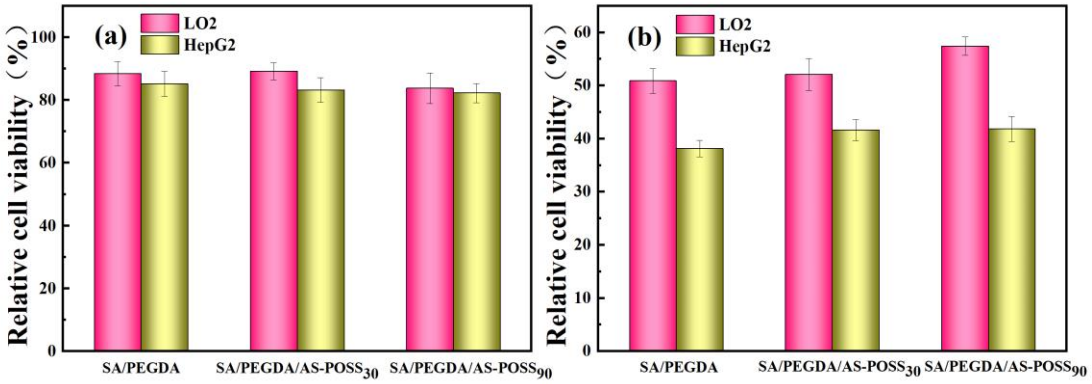

Figure 11. Cell proliferation rate of LO2 and HepG2: (a) drug-free hydrogel; (b) drug-loaded hydrogel.

The hydrogel, as a drug carrier, requires good biocompatibility and low cytotoxicity. To evaluate these properties, MTT assays were performed to test the compatibility of the hydrogel with LO2 (normal liver cells) and HepG2 (tumor liver cells), as presented in Figure 11. The survival rates of HepG2 and LO2 cells cultured with the extract of drug-free hydrogel remain between 80-90% (Figure 11(a)), indicating that the SA/PEGDA/AS-POSS hydrogels has no cytotoxicity and meets the requirements for a drug carrier. In contrast, for drug-loaded hydrogel, the cytotoxicity toward HepG2 cells significantly increased (Figure 11(b)), with the survival rate of HepG2 cells decreasing from approximately 85% to around 40%. The impact on LO2 cells remains much lower than that on HepG2 cells, suggesting that the drug-loaded SA/PEGDA/AS-POSS hydrogels has promising potential as a drug carrier with good prospects for biomedical applications.

4. Conclusion

This work successfully develops SA/PEGDA/AS-POSS hydrogels with enhanced mechanical properties and pH-responsive drug release capabilities. The incorporation of AS-POSS not only improves the swelling behavior and drug loading capacity of the hydrogel but also significantly enhances their mechanical performance. The hydrogel exhibits favorable biocompatibility, showing no toxicity to normal LO2 liver cells, while demonstrating effective cytotoxicity against HepG2 liver cancer cells when loaded with doxorubicin (DOX). Studies on drug release behavior demonstrate that DOX is rapidly released under mildly acidic conditions (pH=6.5), representative of tumor microenvironments, while its release slows significantly under neutral conditions (pH=7.4). This pH-responsive behavior is further supported by the drug release kinetics, which follow Fickian diffusion at pH=6.5 and a non-Fickian mechanism at pH=7.4. Overall, the SA/PEGDA/AS-POSS hydrogels demonstrates promising potential as a drug delivery system, with excellent biocompatibility, improved mechanical strength, targeted drug release, and effectiveness in cancer therapy, making it a highly promising candidate for biomedical applications.

Acknowledgments

The author is very grateful for the support from the National Natural Science Foundation of China (Grant Nos. U1704160, 20804041).

Data availability

Relevant data can be obtained from the author.

References

[1] a) X. Z. Lim, *Chemistry & Industry* **2021**, *85*, 28-31; b) L. J. Li, Y. Liu, X. Y. Tan, F. Teng and Y. Li, *Carbohydrate Polymers* **2025**, *349*; c) B. Darmau, A. Hoang, A. J. Gross and I. Texier, *European Polymer Journal* **2024**, *221*.

[2] a) Y. Zhong, S. H. Zeng, R. H. Su, W. H. Xu, W. W. Zhu, X. C. Tan, K. J. Huang and J. Yan, *Sensors and Actuators B-Chemical* **2025**, *423*; b) N. Wang, Y. M. Zhang, J. Li, H. F. Mao, Q. Zhou, H. Yang, L. J. Wang, Z. Y. Wang, K. Li and X. Q. Yu, *Food Chemistry* **2025**, *464*; c) P. Sakhaii, B. Bohorc, T. Olpp, M. Mohnicke, J. Rieke-Zapp and P. K. Dhal, *Scientific Reports* **2024**, *14*.

[3] X. Y. Zhou, C. K. Wang, Z. F. Shen, Y. F. Wang, Y. H. Li, Y. N. Hu, P. Zhang and Q. Zhang, *Journal of Materials Chemistry B* **2024**, *12*, 7246-7266.
[4] a) M. L. P. Ramos, P. Rivas-Rojas, H. Ascolani, M. Cavallo, F. Bonino, R. F. de Luis, M. X. Guerbi, F. Michelini, C. Bernal, J. M. Lázaro-Martínez and G. Copello, *Materials Chemistry Frontiers* **2024**; b) T. Hemalatha, M. Aarthy, A. Sundarapandiyan and N. Ayyadurai, *Macromolecular Bioscience* **2024**.
[5] a) C. L. Cui, D. Li and L. J. Wang, *Separation and Purification Technology* **2025**, *358*; b) Z. X. Lian, Y. F. Ding, Y. X. Chen, D. Yu and W. Wang, *Colloids and Surfaces a-Physicochemical and Engineering Aspects* **2024**, *703*.
[6] a) J. Parajuli, Y. T. Li, L. K. Chang, L. Y. Ye, Y. C. Han and Y. X. Yin, *Journal of Wuhan University of Technology-Materials Science Edition* **2024**, *39*, 1628-1636; b) W. N. Zhang, H. Wang, J. Pang, Y. D. Huang, H. Li and S. Q. Tang, *International Journal of Biological Macromolecules* **2024**, *278*.
[7] M. R. Rankin, D. Khare, L. Gerwick, D. H. Sherman, W. H. Gerwick and J. L. Smith, *bioRxiv* **2024**.
[8] J. S. Yuan, J. Yu, L. R. Ma, Y. Y. Ma, H. H. Hao, C. Z. Zhao and B. L. Zhou, *Journal of Environmental Chemical Engineering* **2024**, *12*.
[9] Q. Wu, L. Wang, P. Ding, Y. Deng, O. V. Okoro, A. Shavandi and L. Nie, *Composites Communications* **2022**, *35*.
[10] Q. Bai, Q. Gao, F. Hu, C. Zheng, W. Chen, N. Sun, J. Liu, Y. Zhang, X. Wu and T. Lu, *International Journal of Biological Macromolecules* **2023**, *232*.
[11] M. Balakrishnan, V. K. Balasubramanian, K. Murugan, J. Kennedy, J. Y. Chou and J. B. Muthuramalingam, *Materials Today Communications* **2024**, *41*.
[12] J. Song, L. J. Chen, Y. N. Zhou, Z. W. Yuan, Y. H. Niu and Z. Q. Wei, *International Journal of Biological Macromolecules* **2024**, *279*.
[13] a) F. Wajdi and A. E. Tontowi, *Management Systems in Production Engineering* **2024**, *32*, 555-562; b) H. R. Pisheh, A. Sabzevari, M. Ansari and K. Kabiri, *Biopolymers* **2024**; c) R. Kumar, A. Tewari and A. Parashar, *Mechanics of Materials* **2024**, *199*.
[14] a) X. W. Fu, H. Xian, C. L. Xia, Y. Q. Liu, S. Du, B. Wang, P. Xue, B. Wang and Y. J. Kang, *International Journal of Pharmaceutics* **2024**, *666*; b) A. T. D. Lukatsky, Y. V. Dan, L. Mizrahi and E. Amir, *European Polymer Journal* **2024**, *210*; c) A. A. Ashkarran, S. Shari, C. K. Abrahamsson and M. Mahmoudi, *Analytica Chimica Acta* **2022**, *1195*; d) Q. B. Sun, C. P. Xu, W. Q. Li, Q. J. Meng and H. Z. Qu, *Artificial Cells Nanomedicine and Biotechnology* **2021**, *49*, 71-82.
[15] a) Y. Meng, M. Shi, W. Feng, L. Zhang, H. Zhang and X. Zhang, *Journal of Applied Polymer Science* **2024**, *141*; b) C. Yang, H. Huang, S. C. Fan, C. L. Yang, Y. H. Chen, B. Yu, W. Q. Li and J. W. Liao, *Advanced Materials Technologies* **2021**, *6*; c) Y. J. He, T. Jiang, C. Li, C. Zhou, G. C. Yang, J. Q. Nie, F. Y. Wang, C. F. Lu, D. Yin, X. F. Yang and Z. B. Chen, *Polymer Degradation and Stability* **2023**, *211*.
[16] C. Zhou, T. Jiang, S. J. Liu, Y. J. He, G. C. Yang, J. Q. Nie, F. Y. Wang, X. F. Yang, Z. B. Chen and C. F. Lu, *International Journal of Biological Macromolecules* **2024**, *267*.
[17] W. C. Li, M. J. Kong, T. Yang, J. X. Li, H. X. Sun, Z. T. Li, Q. M. Wang and W. Teng, *Chemical Engineering Journal* **2023**, *475*.
[18] K. Q. Fan, S. Liu, W. B. Feng, W. T. Yang, J. W. Peng, R. X. Liu, S. M. Fang and X. J. Zhang, *Journal of Applied Polymer Science* **2024**, *141*.
[19] a) Z. X. Cai, B. Zhang, L. Y. Jiang, Y. Y. Li, G. H. Xu and J. J. Ma, *Progress in Chemistry* **2019**, *31*, 1653-1668; b) D. U. Kapoor, R. Garg, M. Gaur, A. Pareek, B. G. Prajapati, G. R. Castro, S. Suttiruengwong and P. Sriamornsak, *Saudi Pharmaceutical Journal* **2024**, *32*; c) C. Li, X. C. Li, X. P. Liu, L. Yuan, X. Duan and W. Guo, *Colloids and Surfaces B-Biointerfaces* **2025**, *246*.

10.1002/chem.202404538

[20] a) Z. Li, L. Chen, S. Yang, J. Han, Y. Zheng, Z. Chen, X. Shi and J. Yang, *Acta biomaterialia* **2024**; b) J. Zhang, J. Liu, S. He, Z. Y. Cui and W. Shao, *Colloids and Surfaces a-Physicochemical and Engineering Aspects* **2023**, *674*.